Vol.3, No.9, 537-541 (2011)
doi:10.4236/health.2011.39090



# Relationship between work style and cigarette smoking in Japanese workers

**Nobuyuki Miyatake[1*], Kenji Nishii[2], Takeyuki Numata[3]**

[1]Department of Hygiene, Faculty of Medicine, Kagawa University, Kagawa, Japan;
*Corresponding Author: miyarin@med.kagawa-u.ac.jp
[2]Okayama Health Foundation Hospital, Okayama Health Foundation, Okayama, Japan;
[3]Okayama Southern Institute of Health, Okayama Health Foundation, Okayama, Japan.

Received 30 June 2011; revised 1 August 2011; accepted 9 August 2011.

## ABSTRACT

**We investigated the link between work style (*i.e.* day work and shift work) and cigarette smoking in Japanese workers. We used data of 3,238 men (39.3 ± 10.5 years) and 5,111 women (37.1 ± 10.9 years), aged 20 - 59 years, by cross-sectional clinical investigation study. Work style *i.e.* day work and shift work, cigarette smoking, status of stress and stress coping were obtained by questionnaires by well-trained medical staff. A total of 227 men (7.0%) and 339 women (6.6%) were shift workers, and 1346 men (41.6%) and 649 women (12.7%) were current smokers. Work style was significantly linked to cigarette smoking, stress and stress coping after adjusting for age in women. In addition, the level of stress coping in subjects with cigarette smoking was significantly lower than that in subjects without cigarette smoking even after adjusting for age in women. However, these associations were not noted in men. Work style was critically associated with cigarette smoking in Japanese female workers.**

**Keywords:** Work Style; Shift Work; Cigarette Smoking; Stress Coping

## 1. INTRODUCTION

Economic globalization needs continuous processing or operations around the clock to optimize manufacturing system. A 24-hour continuous operation system has become more popular and shift workers have become also more popular in Japan. Several reports have showed that shift work is associated with coronary artery disease [1], hyper cholesterolemia [2,3], weight gain [4] and hypertension [5].

Cigarette smoking is an important public health challenge, and it has been reported that 39.4% of men and 11.0% of women are current smokers in Japan [6]. Cigarette smoking is also a strong risk factor for atherosclerosis and cardiovascular disease in a dose-dependent manner [7]. However, the link between work style such as day work and shift work, and cigarette smoking in Japanese workers still remains to be investigated.

Therefore, in this study, we evaluated the link between work style and cigarette smoking and the effect of stress and stress coping on cigarette smoking in Japanese workers.

## 2. SUBJECTS AND METHODS

### 2.1. Subjects

We used data for 3238 Japanese male workers (39.3 ± 10.5 years) and 5111 women (37.1 ± 10.9 years), retrospectively from a database of 16,380 subjects who met the following criteria: 1) they had wanted to change their lifestyle *i.e.* diet and exercise habits, and had received an annual health check-up from June 1997 to Dec 2009 at Okayama Southern Institute of Health, 2) received evaluation of work style, cigarette smoking, status of stress and stress coping as part of the annual health check-up, 3) they were day workers and/or shift workers, aged 20 - 59 years, and 4) provided written informed consent (**Table 1**).

Ethical approval for the study was obtained from the Ethical Committee of Okayama Health Foundation.

### 2.2. Work Style

Subjects completed a self-administered questionnaire. This included the following question regarding patterns of work style: During your working life, until the present, what shift (time of day) did you work most: mainly day time, mainly night (*i.e.* fixed-night shift), or alternate

**Table 1.** Clinical profiles of enrolled subjects.

| | Men | Women |
|---|---|---|
| Number of subjects | 3238 | 5111 |
| Age | 39.3 ± 10.5 | 37.1 ± 10.9 |
| Height (cm) | 167.0 ± 5.8 | 157.2 ± 5.4 |
| Body weight (kg) | 71.2 ± 11.7 | 54.8 ± 9.2 |
| Body mass index (kg/m$^2$) | 24.6 ± 3.7 | 22.2 ± 3.6 |
| Abdominal circumference (cm) | 83.9 ± 10.2 | 70.3 ± 9.2 |
| Hip circumference (cm) | 94.6 ± 6.2 | 91.0 ± 6.1 |
| | | Mean ± SD |

night and daytime (that is, rotating-shift work)? In this study, we excluded 65 male and 131 female night workers to evaluate the influence of shift work on cigarette smoking compare to day workers.

## 2.3. Exposure Data

The self-administered questionnaire also inquired about other characteristics of smoking status (never or current smoker), status of stress (yes or no) and stress coping (yes or no).

## 2.4. Anthropometric Measurements

The anthropometric parameters were evaluated by using the following respective parameters such as height, body weight, body mass index (BMI), abdominal circumference, hip circumference. BMI was calculated by weight/[height]$^2$ (kg/m$^2$). The abdominal circumference was measured at the umbilical level and the hip was measured at the widest circumference over the trochanter in standing subjects after normal expiration [8].

## 2.5. Statistical Analysis

Data are expressed as mean ± standard deviation (SD) values. A comparison of parameters was performed by $\chi^2$ test and logistic regression analysis: $p < 0.05$ was considered to be statistically significant. Statistical analysis was performed with StatView 5.0 (SAS Institute Inc., Cary, NC, USA).

# 3. RESULTS

A total of 227 men (7.0%) and 339 women (6.6%) were shift workers, and the rate of shift workers was the highest in 20's in both sexes (**Table 2**).

**Table 3** shows the comparison of cigarette smoking as classified by age group. Current smokers were decreased with age in both sexes, and 1346 men (41.6%) and 649 women (12.7%) were current smokers.

We also evaluated the status of stress (**Table 4**). 2071 men (64.0%) and 3,735 women (73.1%) women answered as having stress, and the rate of subjects with having stress was the highest in 30's in both sexes. However, subjects with having stress coping was comparably lower [1539 men (47.5%) and 2730 women (53.5%)] (**Table 5**). The rate of subjects with having stress coping was the highest in 20's in men and in 50's in women.

In addition, we evaluated the relationship between work style and cigarette smoking, status of stress and stress coping. In women, the rate of current smoker and having stress was significantly higher in shift workers than those in day workers after adjusting for age (**Table 6**). The rate of having stress coping in shift workers was significantly higher than that in day workers after adjusting for age. In men, those clear associations were not noted.

Finally, we investigated the relationship between cigarette smoking and status of stress and stress coping (**Table 7**). The rate of having stress coping in current smokers was significantly lower than that in non smokers even after adjusting for age in women, but not in men. The relationship between cigarette smoking and status of stress was not noted in both sexes.

# 4. DISCUSSION

We evaluated the link between work style and cigarette smoking in Japanese workers and we found that close associations between shift work and cigarette smoking in female workers. In addition, having stress coping might be important for Japanese female workers for prohibiting smoking.

In some literatures, work style was closely associated with cigarette smoking especially male workers. Fujino *et al.* reported that the rate of current smoker was higher in shift male workers (59.5%) than that in day male workers (55.4%) in Japan Collaborative Cohort Study for the Evaluation of Cancer Risk (JACC Study) [1]. Dochi *et al.* also reported that the rate of current smoker was higher in shift workers (68.8%) than that in day workers (58.8%) in male workers in steel company [2]. Suwazono *et al.* also showed that shift work was closely associated with cigarette smoking in male workers [4]. There were few studies that evaluated the relationship between shift work and cigarette smoking in Japanese female workers. Kageyama *et al.* reported that the prevalenve of current smoker was 29%, being higher than that in the general population of Japanese women by evaluating 522 Japanese female staff nurses [9]. In this study, it is note worthy that we found the relationship between work style and cigarette smoking in women

 

even after adjusting for age. However, those associations were not noted as previous study in men. Enrolled subjects in this study were undertaken health check-up and they wanted to change their lifestyle. Therefore close associations might not be noted in men.

According to the relation between work style and status of stress, 3-shift system of employment increases work-related stress [10]. Parkes carried out cross-sectional

**Table 2.** Comparison of work style as classified by age group.

| | Men | | | | Women | | | |
|---|---|---|---|---|---|---|---|---|
| | Day work | % | Shift work | % | Day work | % | Shift work | % |
| 20 - 29 | 661 | 90.4 | 70 | 9.6 | 1575 | 90.0 | 175 | 10.0 |
| 30 - 29 | 888 | 92.6 | 71 | 7.5 | 1135 | 93.5 | 79 | 6.5 |
| 40 - 49 | 790 | 93.7 | 53 | 6.3 | 1207 | 95.3 | 59 | 4.7 |
| 50 - 59 | 672 | 95.3 | 33 | 4.7 | 855 | 97.0 | 26 | 3.0 |
| Total | 3011 | 93.0 | 227 | 7.0 | 4772 | 93.4 | 339 | 6.6 |

**Table 3.** Comparison of cigarette smoking as classified by age group.

| | Men | | | | Women | | | |
|---|---|---|---|---|---|---|---|---|
| | Cigarette smoking (+) | % | Cigarette smoking (–) | % | Cigarette smoking (+) | % | Cigarette smoking (–) | % |
| 20 - 29 | 329 | 45.0 | 402 | 55.0 | 281 | 16.1 | 1469 | 83.9 |
| 30 - 29 | 413 | 43.1 | 546 | 56.9 | 179 | 14.7 | 1035 | 85.3 |
| 40 - 49 | 349 | 41.4 | 494 | 58.6 | 130 | 10.3 | 1136 | 89.7 |
| 50 - 59 | 255 | 36.2 | 450 | 63.8 | 59 | 6.7 | 822 | 93.3 |
| Total | 1346 | 41.6 | 1892 | 58.4 | 649 | 12.7 | 4462 | 87.3 |

**Table 4.** Comparison of stress as classified by age group.

| | Men | | | | Women | | | |
|---|---|---|---|---|---|---|---|---|
| | Stress (+) | % | Stress (–) | % | Stress (+) | % | Stress (–) | % |
| 20 - 29 | 443 | 60.6 | 288 | 39.4 | 1297 | 74.1 | 453 | 25.9 |
| 30 - 29 | 645 | 67.3 | 314 | 32.7 | 925 | 76.2 | 289 | 23.8 |
| 40 - 49 | 566 | 67.1 | 277 | 32.9 | 910 | 71.9 | 356 | 28.1 |
| 50 - 59 | 417 | 59.1 | 288 | 40.9 | 603 | 68.4 | 278 | 31.6 |
| Total | 2071 | 64.0 | 1167 | 36.0 | 3735 | 73.1 | 1376 | 26.9 |

**Table 5.** Comparison of stress coping as classified by age group.

| | Men | | | | Women | | | |
|---|---|---|---|---|---|---|---|---|
| | Stress coping (+) | % | Stress coping (–) | % | Stress coping (+) | % | Stress coping (–) | % |
| 20 - 29 | 377 | 51.6 | 354 | 48.4 | 957 | 54.7 | 793 | 45.3 |
| 30 - 29 | 419 | 43.7 | 540 | 56.3 | 642 | 52.9 | 572 | 47.1 |
| 40 - 49 | 405 | 48.0 | 438 | 52.0 | 631 | 49.8 | 635 | 50.2 |
| 50 - 59 | 338 | 47.9 | 367 | 52.1 | 500 | 56.8 | 381 | 43.1 |
| Total | 1539 | 47.5 | 1699 | 52.5 | 2730 | 53.4 | 2381 | 46.6 |

**Table 6.** Relationship between work style and cigarette smoking, stress and stress coping.

| **Men** | Cigarette smoking (+) | Cigarette smoking (–) | *p* | *p* (After adjusting for age) |
|---|---|---|---|---|
| Day work | 1248 | 1763 | 0.6113 | 0.7664 |
| Shift work | 98 | 129 | | |
| | Stress (+) | Stress (–) | | |
| Day work | 1924 | 1087 | 0.7950 | 0.8360 |
| Shift work | 147 | 80 | | |
| | Stress coping (+) | Stress coping (–) | | |
| Day work | 1419 | 1592 | 0.0951 | 0.1054 |
| Shift work | 120 | 107 | | |
| **Women** | Cigarette smoking (+) | Cigarette smoking (–) | | |
| Day work | 574 | 4198 | **<0.0001** | **<0.0001** |
| Shift work | 75 | 264 | | |
| | Stress (+) | Stress (–) | | |
| Day work | 3444 | 1328 | **<0.0001** | **<0.0001** |
| Shift work | 291 | 48 | | |
| | Stress coping (+) | Stress coping (–) | | |
| Day work | 2505 | 2267 | **<0.0001** | **<0.0001** |
| Shift work | 225 | 114 | | |

**Table 7.** Relationship between cigarette smoking and stress, stress coping.

| **Men** | Stress (+) | Stress (–) | *p* | *p* (After adjusting for age) |
|---|---|---|---|---|
| Cigarette smoking (+) | 840 | 506 | 0.1208 | 0.1053 |
| Cigarette smoking (–) | 1231 | 661 | | |
| | Stress coping (+) | Stress coping (–) | | |
| Cigarette smoking (+) | 602 | 744 | **0.0070** | 0.1054 |
| Cigarette smoking (–) | 937 | 955 | | |
| **Women** | Stress (+) | Stress (–) | | |
| Cigarette smoking (+) | 496 | 153 | **0.0396** | 0.0797 |
| Cigarette smoking (–) | 3239 | 1223 | | |
| | Stress coping (+) | Stress coping (–) | | |
| Cigarette smoking (+) | 321 | 328 | **0.0307** | **<0.0001** |
| Cigarette smoking (–) | 2409 | 2053 | | |

research targeting 736 two-shift workers and 1131 day workers at an oil refinery, and concluded that the 2-shift workers had higher job demand and less job control over their work [11]. In female workers, Kageyama *et al.* reported that the cigarette smoking-dependent tendency was associated with recent life events and the presence of insomnia [9]. Stress is probably the most important contributor to excess smoking levels [12]. American study showed that officers who smoked experienced high-stress levels more than twice that of non smokers [13]. Therefore, stress coping may important for prohibiting cigarette smoking. Serxner *et al.* recommended that

 

smoking cessation and prevention programs should focus on change in individual coping mechanisms [14]. We also found that the rate of stress in shift smokers was higher than that in day workers and the rate of stress coping was also higher in shift workers than that in day workers after adjusting in women. Although the rate of stress coping was higher in shift workers than that in day workers, the rate of stress coping was significantly lower than in current smokers than that in non smokers in women. Taken together, it seems reasonable to suggest that simply recommending proper stress coping except cigarette smoking, might result in decreased cigarette smoking in some Japanese female workers.

Potential limitations remain in this study. First, our study was a cross sectional and not a longitudinal study. Second, the 3238 Japanese male workers and 5111 women, all of whom wanted to change their lifestyle, underwent measurements for this study: they were therefore more health-conscious than the average person. In fact, in men, clear associations were not noted the relationship between shift work and cigarette smoking as previous studies [1,2,4]. Third, we could not obtain the data of the average number of cigarettes smoked per day or subject' age when they started smoking. Subjects who smoked before the date of the analysis but who had stopped by then would have therefore been categorized as non-smokers. Fourth, status of stress and stress coping was evaluated by simple questionnaire (yes or no). Therefore, further prospective studies are needed in Japanese workers to prove the link between work style and cigarette smoking.

## 5. CONFLICT OF INTEREST

There is no conflict of interest.

## REFERENCES


[1] Fujino, Y., Iso, H., Tamakoshi, A., Ishiba, Y., Koizumi, A., Kubo, T. and Yoshimura, T. (2006) Japanese Collaborative Cohort Study Group: A prospective cohort study of shift work and risk of ischemic heart disease in Japanese male workers. *American Journal of Epidemiology*, **164**, 128-135. doi:10.1093/aje/kwj185

[2] Dochi, M., Sakata, K., Oishi, M., Tanaka, K., Kobayashi, E. and Suwazono, Y. (2008) Relationship between shif work and hyper cholesterolemia in Japan. *Scandinavian Journal of Work, Environment & Health*, **34**, 33-39.

[3] Dochi, M., Suwazono, Y., Sakata, K., Okubo, Y., Oishi, M., Tanaka, K., Kobayashi, E. and Nogawa, K. (2009) Shift work is a risk factor for increased total cholesterol level: A 14-year prospective cohort study in 6886 male workers. *Occupational and Environmental Medicine*, **66**, 592-597. doi:10.1136/oem.2008.042176

[4] Suwazono, Y., Dochi, M., Sakata, K., Okubo, Y., Oishi, M., Tanaka, K., Kobayashi, E., Kido, T. and Nogawa, K. (2008) A longitudinal study on the effect of shift work on weight gain in male Japanese workers. *Obesity (Silver Spring)*, **16**, 1887-1893. doi:10.1038/oby.2008.298

[5] Suwazono, Y., Dochi, M., Sakata, K., Okubo, Y., Oishi, M., Tanaka, K., Kobayashi, E. and Nogawa, K. (2008) Shift work is a risk factor for increased blood pressure in Japanese men: A 14-year historical cohort study. *Hypertension*, **52**, 581-586. doi:10.1161/HYPERTENSIONAHA.108.114553

[6] The National Nutrition Survey in Japan (2010). http://www.mhlw.go.jp/houdou/2008/12/dl/h1225-5j.pdf

[7] Peto, R. (1994) Smoking and death: The past 40 years and the next 40. *British Medical Journal*, **209**, 937-939.

[8] Anonym (2005) Definition and the diagnostic standard for metabolic syndrome—Committee to Evaluate Diagnostic Standards for Metabolic Syndrome. *Nippon Naika Gakkai Zasshi*, **94**, 794-809. doi:10.2169/naika.94.794

[9] Kageyama, T., Kobayashi, T., Nishikido, N., Oga, J. and Kawashima, M. (2005) Associations of sleep problems and recent life events with smoking behaviors among female staff nurses in Japanese hospitals. *Industrial Health*, **43**, 133-141. doi:10.2486/indhealth.43.133

[10] Harada, H., Suwazono, Y., Sakata, K., Okubo, Y., Oishi, M., Uetani, M., Kobayashi, E. and Nogawa, K. (2005) Three-shift system increases job-related stress in Japanese workers. *Journal of Occupational Health*, **47**, 397-404. doi:10.1539/joh.47.397

[11] Parkes, K.R. (2003) Shift work and environment as interactive predictors of work perceptions. *Journal of Occupational Health Psychology*, **8**, 266-281. doi:10.1037/1076-8998.8.4.266

[12] Smith, D.R., Devine, S., Leggat, P.A. and Ishitake, T. (2005) Alcohol and tobacco consumption among police officers. *Kurume Medical Journal*, **52**, 63-65. doi:10.2739/kurumemedj.52.63

[13] Kohan, A. and O'Connor, B.P. (2002) Police officer job satisfaction in relation to mood, well-being, and alcohol consumption. *The Journal of Psychology*, **136**, 307-318.

[14] Serxner, S., Catalano, R., Dooley, D. and Mishra, S. (1991) Tobacco use: Selection, stress, or culture? *Journal of Occupational Medicine*, **33**, 1035-1039.


 

# Influence of Slice Thickness on Diagnoses of Pulmonary Nodules Using Low-dose CT:

## *Potential Dependence of Detection and Diagnostic Agreement on Features and Location of Nodule*

Marodina Sinsuat, MS, Shinsuke Saita, PhD, Yoshiki Kawata, PhD, Noboru Niki, PhD, Hironobu Ohmatsu, MD, Takaaki Tsuchida, MD, Ryutaro Kakinuma, MD, Masahiko Kusumoto, MD, Kenji Eguchi, MD, Masahiro Kaneko, MD, Hiroshi Morikubo, MD, Noriyuki Moriyama, MD, PhD

**Rationale and Objectives:** The aims of this study were to assess the influence of slice thickness on the ability of radiologists to detect or not detect nodules and to agree or disagree on the diagnosis and also to investigate the potential dependence of these relations on the sizes, average computed tomographic (CT) values, and locations of the nodules.

**Materials and Methods:** Six radiologists performed qualitative diagnostic readings of multislice CT images with a slice thickness of 2 or 10 mm obtained from 360 subjects. The nodules were diagnosed as nodules for further examination (NFEs), inactive nodules for no further examination (INNFEs), or no abnormality. The results of the diagnoses were cross-tabulated and quantitatively analyzed using the average CT values, sizes, and locations of the nodules with reference to the 2-mm slices. Multivariate logistic regression analyses were used to estimate the significant associations of these parameters with the ability of radiologists to detect or not detect nodules and to agree or disagree on the diagnosis.

**Results:** Totals of 130 NFEs and 403 INNFEs for 2-mm slice thickness and 142 NFEs and 338 INNFEs for 10-mm slice thickness were diagnosed. Nodule classifications were as follows: the same diagnosis on both slice thickness images (67.6%), different diagnoses on two slice thickness images (21%), missed on 10-mm slice thickness images (10.6%), and misinterpreted on 10-mm slice thickness images (0.7%). Regarding detection and nondetection, NFE diagnoses were influenced by size (odds ratio [OR], 132.50; 95% confidence interval [CI], 4.77–4711) and the average CT value (OR, 27.20; 95% CI, 3.21–645.3), and INNFE diagnoses were influenced by size (OR, 16.10; 95% CI, 6.18–55.19) and the average CT value (OR, 7.67; 95% CI, 2.19–30.91). Regarding diagnostic agreement and disagreement, the NFE diagnoses were influenced by size (OR, 3.60; 95% CI, 1.29–11.04), nodule distance from the lung border (OR, 2.85; 95% CI, 1.27–6.65), and nodule location in the right upper lobe (OR, 0.07; 95% CI, 0.003–0.477), while the INNFE diagnoses were influenced by the average CT value (OR, 11.84; 95% CI, 3.33–55.86), size (OR, 0.42; 95% CI, 0.25–0.70), and nodule distance from the lung border (OR, 0.41; 95% CI, 0.25–0.66).

**Conclusions:** The influence of slice thickness on the ability of radiologists to detect or not detect nodules and to agree or disagree on the diagnosis was quantitatively evaluated. Detection and nondetection of NFEs and INNFEs are influenced by size and average CT value. Agreement and disagreement on NFE and INNFE diagnoses are influenced not only by size and average CT value but also, importantly, by the locations of nodules.

**Key Words:** Slice thickness; pulmonary nodules; detection; agreement; computed tomography.



Lung cancer has the highest mortality rate of all cancers in Japan. Early detection is necessary to improve the prognosis of this disease. For this reason, several lung cancer screening programs have been conducted (1–3). The modalities used for lung cancer screening include chest x-ray, sputum cytology, low-dose x-ray helical computed tomographic (CT) imaging, and multislice CT (MSCT) imaging (2). Compared to other modalities, CT imaging excels in the imaging of the lungs; therefore, several programs have adopted CT imaging as the modality of choice for lung cancer screening (4). Recently, Henschke and Yankelevitz (5) provided an update of CT screening for lung cancer in 2007. This update summarizes the diagnostic and prognostic measures available for screening trials to date.

Henschke et al (6) also reported the baseline findings from the Early Lung Cancer Action Project, in which low-dose helical CT scans were performed using 10-mm slice thickness.

**Acad Radiol 2011;** 18:594–604

From Functional Systems Engineering (M.S.) and the Institute of Technology and Science (S.S., Y.K., N.N.), University of Tokushima, 770-8506, Minamijosanjima-cho, 2-1, Tokushima, Japan; National Cancer Center Hospital East, Kashiwa, Japan (H.O.); National Cancer Center Hospital, Tokyo, Japan (T.T., M. Kusumoto, M. Kaneko); the National Cancer Center Research Center for Cancer Prevention and Screening, Tokyo, Japan (R.K., N.M.); the School of Medicine, Teikyo University, Tokyo, Japan (K.E.); and Tochigi Public Health Service Association, Utsunomiya, Japan (H.M.). Received September 29, 2010; accepted January 14, 2011. **Address correspondence to:** Y.K. e-mail: kawata@opt.tokushima-u.ac.jp


doi:10.1016/j.acra.2011.01.007

Currently, baseline and repeat screenings are being performed using MSCT scanners with 1.25-mm slice thickness (7). Moreover, Swensen et al (8) reported lung cancer CT screening using 5-mm slice thickness, and images with slice thicknesses of 1 to 3 mm are currently being used at the Mayo Clinic.

In Japan, low-dose helical CT screening was introduced by the Anti–Lung Cancer Association in 1993, and MSCT screening was started in 2002 (9). One study performed 3457 low-dose helical CT examinations using 10-mm slice thickness (3). From 1996 to 1998, Sone et al (2) performed population-based annual lung cancer screening using low-dose helical CT scanning with 10-mm slice thickness; these investigators are currently using 5-mm slice thickness. From 2001 to 2002, Nawa et al (10) reported the results of CT screening performed on 7956 participants who belonged to the Hitachi Employees' Health Insurance Group using 10-mm slice thickness; these investigators are currently using 5-mm slice thickness. In 2004, the Research Center for Cancer Prevention and Screening of the National Cancer Center began to use MSCT screening with 2-mm and a 5-mm slice thicknesses (9). Until now, no standard slice thickness has been set, and each institution uses a slice thickness ranging from 1 to 10 mm.

In 2005, MacMahon et al (11) reported recommendations for the management of small pulmonary nodules detected on CT scans, with reference to a statement from the Fleischner Society. The Anti–Lung Cancer Association followed certain qualitative criteria for diagnosis using lung cancer CT screening with 10-mm slice thickness (1). The Japanese Society of CT Screening (12) subsequently quantified these criteria.

Thick-section images (10-mm slice thickness) were initially used, while thin-section images are mostly used at present. To date, only a few studies have documented the influence of slice thickness on the diagnosis of pulmonary nodules (13–16).

In this study, we assessed the influence of 2-mm slice thickness (thin section) and 10-mm slice thickness (thick section) on the ability of radiologists to detect or not detect nodules and to agree or disagree on the diagnosis and investigated the potential dependence of these relations on the sizes, average CT values, and locations of the nodules. The detection or nondetection of nodules for further examination (NFEs) and inactive nodules for no further examination (INNFEs) were influenced by nodule size and average CT value. Agreement and disagreement regarding NFE and INNFE diagnoses were influenced not only by the nodule size and average CT value but also, importantly, by the locations of the nodules.

## MATERIALS AND METHODS

This retrospective study was approved by the institutional review board; the requirement for patient informed consent was waived.

### *MSCT Images*

Lung cancer MSCT screening was conducted in 360 consecutive participants (236 men, 124 women) at the Tochigi Public Health Service Association between September 2000 and September 2001. Of this number, four cases of lung cancer were diagnosed. The mean ages of the subjects were 53.6 years (range, 28–76 years) for men and 52.4 years (range, 35–75 years) for women. The CT scanner used for the screening was a Toshiba Aquilion (Toshiba Medical Systems, Inc, Otawara, Japan), and the scanning parameters were 120 kV, 30 mA, 0.5-second scanning time, 2 mm × 4, and a helical pitch of 5.5. A tube current of 30 mA results in a low dose of radiation to the patient. Using these parameters, the effective dose was calculated using effective dose calculation software, a combination of NRPB2501 and the ImPACT CT Patient Dosimetry Calculator 2 (17,18). The effective dose was 0.71 mSv, and lung dose was 1.8 mSv. Two kinds of reconstruction images were created: 2-mm slice thickness and a 2-mm reconstruction interval, and 10-mm slice thickness and a 10-mm reconstruction interval. The reconstruction function was FC10, the pixel size was 0.5 to 0.686 mm, and the pixel image size was 512 × 512.

### *Qualitative Diagnostic Readings*

Diagnostic readings were made by six radiologists (H.O., R.K., T.T., M. Kusumoto, K.E., and M. Kaneko), each with 19 to 28 years of experience in the diagnostic field and about 16 years of experience with CT screening. The display conditions for the diagnostic readings were a window of 1500 Hounsfield units and a window level of −500 HU. The images were displayed on a Totoku CCL 316 flat-panel 24-bit color monitor (Totoku Corporation, Tokyo, Japan) with 2048 × 1536 resolution. The main objective of the diagnostic reading was to classify the nodules into three categories. The diagnostic reading criteria for each of these categories are shown in Table 1 (12). For NFEs, further examinations were usually performed using follow-up CT imaging, magnified CT images, dynamic contrast-enhanced CT imaging, positron emission tomography, and/or biopsy. For INNFEs, the nodules were reexamined during subsequent screening examinations.

The 2-mm and 10-mm slice thickness images were given to the radiologists for a double diagnostic reading, consisting of an individual reading and a group consensus reading. For the individual reading, the six radiologists were given the 2-mm and 10-mm slice thickness images obtained from 360 subjects. Each radiologist was allotted 60 CT examinations of 2-mm slice thickness and 60 CT examinations of 10-mm slice thickness. The CT examinations were distributed in such a way that each radiologist would not read the 2-mm and the 10-mm slice thickness images from the same subject. For the group consensus readings, the radiologists were grouped into two groups of three radiologists each. Each member of the group reevaluated his own diagnosis of the 2-mm and 10-mm slice thickness images. The results of the group consensus were regarded as the final diagnoses.

### *Cross-tabulation of Diagnosed Nodules*

The radiologists' actual diagnoses using the 2-mm and 10-mm slice thickness images were cross-tabulated. On the basis of the

**TABLE 1. Diagnostic Criteria for Pulmonary Nodule Diagnosis**

A nodule >3 mm in diameter
A nodule characterized as
1. Nodule for further examination
   - Suspected lung cancer
   - Suspected disease other than lung cancer such as tuberculosis, inflammation, scar, and granuloma
2. Inactive nodule for no further examination
   - With areas of opacification with calcification
   - With multiple lesions confined to the same segment
   - With a polygonal shape
   - With linear shadows of focally collapsed lung
3. No abnormality
   - Diagnosed as normal

cross-tabulation results, the pulmonary nodules were classified into four groups: nodules with the same diagnosis for the 2-mm and the 10-mm slice thickness images, nodules with different diagnoses for the 2-mm and the 10-mm slice thickness images, nodules that were missed on the 10-mm slice thickness images, and nodules that were misinterpreted on the 10-mm slice thickness images.

### *Nodule Detection and Nondetection and Diagnostic Agreement and Disagreement*

Using the cross-tabulation results, nodule detection and diagnostic agreement were analyzed. Detection was regarded as nodules that were detected using the 10-mm slice thickness images among the nodules that were detected using the 2-mm slice thickness images. Nondetection was regarded as nodules that were detected using the 2-mm slice thickness images but not using the 10-mm slice thickness images. Agreement was regarded as nodules of the same diagnoses for both the 2-mm and 10-mm slice thickness images. Disagreement was regarded as nodules of different diagnoses for the 2-mm and 10-mm slice thickness images.

### *Quantitative Analysis of Diagnosed Nodule Features and Locations*

We performed a quantitative evaluation of the nodules using 2-mm slice thickness images. To measure the size and average CT values, a semiautomated extraction procedure was carried out. The semiautomated extraction was performed using the following procedures. Three cross-sectional images (transverse, coronal, and sagittal) were simultaneously observed at an interactively selected location. These images were displayed with a window level of −500 HU and a window width of 1500 HU, the same conditions as those used for the diagnostic readings. The lung volume extraction was automatically performed. The background bias included in the lung area was corrected (19). The nodule volumes were segmented using a single fixed-threshold approach and a three-dimensional connected component analysis. Attachments to the nodule volume, such as vessels or bronchioles, were removed using a three-dimensional morphologic opening operation. The consistency of the segmentation results was visually inspected by the operators (Y.K. and N.N., with 15 and 20 years of experience with chest image analysis, respectively). If any of the nodule segmentation results were considered suboptimal, the nodule contours were superimposed on the original images and interactively corrected by the operators. Two different cases require interactive correction: (1) nodules needing a change in the selected threshold value to contain a nonsolid region with a lower value than the threshold value and (2) nodules needing manual separation from the surrounding structures, such as the pleura, mediastinum, or diaphragm (20). The size was defined as the average length and width of the nodule on the transverse image with the largest cross-sectional area, and the average CT value was calculated for the largest cross-sectional area. We also determined the location in the lung lobe using the lung lobe classification algorithm developed in our laboratory. Algorithms for lung lobe classification and the measurement of the distance from the lung border are shown in Figure 1 (21,22).

The 2-mm slice thickness images of nodules located within 3 mm of the lung border are shown in Figure 2.

### *Statistical Analysis*

A multivariate logistic regression analysis was performed to control for confounding parameters associated with detection or nondetection and diagnostic agreement or disagreement. We used size, average CT value, location in the lung lobe, and distance from the lung border as parameters. The goodness of fit for the model was assessed by using the Hosmer-Lemeshow test (23). The analysis was performed for the NFE and INNFE diagnoses using the 2-mm slice thickness results. The data were entered into R version 2.10.1 (The R Project for Statistical Computing, Vienna, Austria), and differences with $P$ values $< .05$ were regarded as significant.

## RESULTS

### *Diagnostic Reading and Nodule Groupings*

We performed a cross-tabulation of the physicians' actual diagnoses using the 2-mm and 10-mm slice thickness images of the pulmonary nodules, as shown in Table 2. Of the total number of NFEs, four cases of lung cancer (3% and 2.8%) were diagnosed on both the 2-mm and the 10-mm slice thickness images, respectively. The number of nodules diagnosed using the 2-mm slice thickness images was 11% higher, but the number of NFE diagnoses was 8% lower than the number of nodules diagnosed using the 10-mm slice thickness images. Using the cross-tabulation results, the nodules were classified into four groups, as shown in Table 3.

### *Quantitative Analysis*

Figure 3 shows images from the first group of diagnosed nodules: (1) four lung cancer cases, depicted as NFEs, and

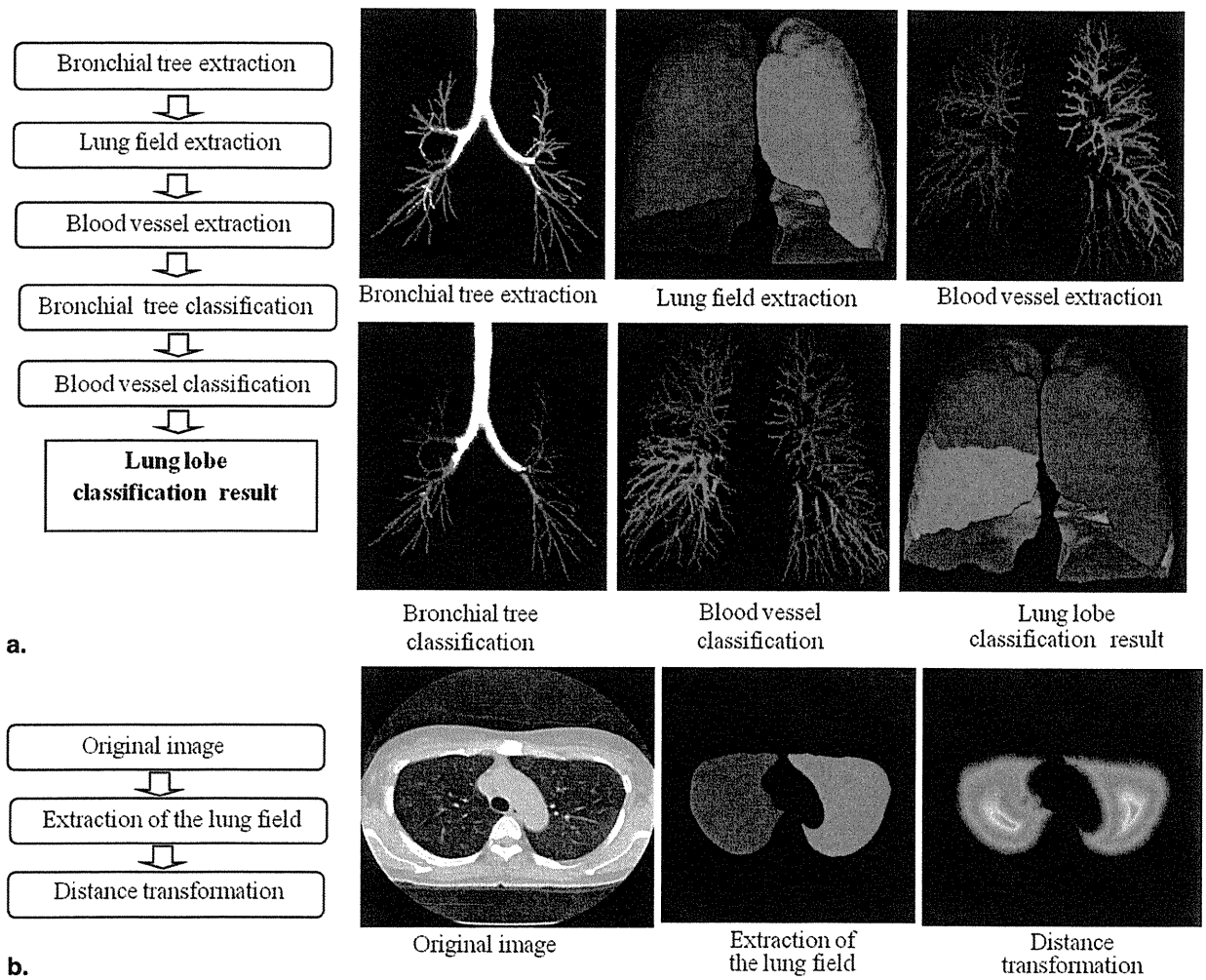


**Figure 1.** Algorithms for lung lobe classification **(a)** and measurement of distance from the lung border **(b)**.

(2) four INNFEs. Figure 4a shows a scatterplot of the average CT values and sizes of the 2-mm NFE, 10-mm NFE nodules and the 2-mm INNFE, 10-mm INNFE nodules. On the scatterplot, the vertical line denotes the minimum average CT value (−820 HU), and the horizontal line denotes the minimum nodular size of 2.5 mm. The 2-mm NFE, 10-mm NFE nodules and the 2-mm INNFE, 10-mm INNFE nodules are differentiated by the demarcation line shown on the scatterplot.

Figure 5 shows images of nodules with different diagnoses for the 2-mm and 10-mm slice thickness images: (1) 2-mm NFE, 10-mm INNFE nodules and (2) 2-mm INNFE, 10-mm NFE nodules. Figure 4b shows a scatterplot of the average CT values and sizes; both the 2-mm NFE, 10-mm INNFE nodules and the 2-mm INNFE, 10-mm NFE nodules were clustered above the demarcation line, although some 2-mm INNFE, 10-mm NFE nodules were found below or near the demarcation line.

Figure 6 shows images of nodules that were missed on the 10-mm slice thickness images: (1) 2-mm NFE, 10-mm no abnormality (NA) nodules and (2) 2-mm INNFE, 10-mm NA nodules. Figure 4c shows a scatterplot of the average CT values and sizes; the 2-mm NFE, 10-mm NA nodules were found above the demarcation line except for one nodule, and all of these lesions had low average CT values and small sizes, while the 2-mm INNFE, 10-mm NA nodules were found mostly below the demarcation line.

The nodules that were misinterpreted on the 10-mm slice thickness images were the 2-mm NA, 10-mm NFE nodules and the 2-mm NA, 10-mm INNFE nodules. In these cases, blood vessels were misinterpreted as nodules on the 10-mm slice thickness images.

Of a total of 537 nodules, 186, 33, 107, 105, and 106 nodules were located in the right upper lobe, right middle lobe, right lower lobe, left upper lobe, and left lower lobe, respectively. These findings indicate that 35% of

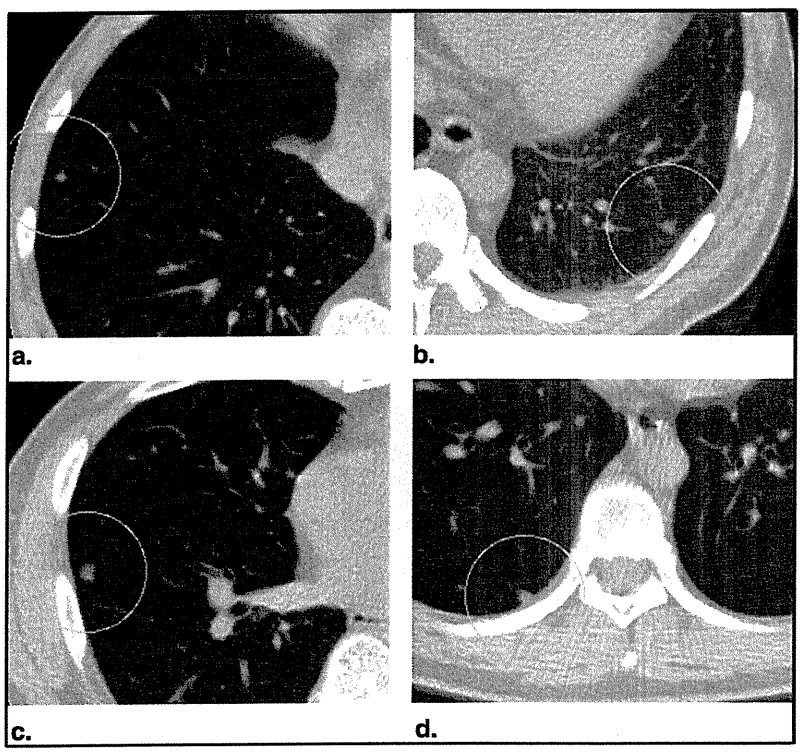


**Figure 2.** Images of nodules located within 3 mm of the lung border. **(a)** A 2-mm NFE, 10-mm INNFE nodule in the right middle lobe at a distance of 3.1 mm from the lung border. **(b)** A 2-mm NFE, 10-mm INNFE nodule located in the left lower lobe at a distance of 2.5 mm from the lung border. **(c)** A 2-mm NFE, 10-mm INNFE nodule located in the right lower lobe at a distance of 1.3 mm from the lung border. **(d)** A 2-mm INNFE, 10-mm NFE nodule located in the right lower lobe in direct contact with the lung border. INNFE, inactive nodule for no further examination; NFE, nodule for further examination.

**TABLE 2. Cross-tabulation of Pulmonary Nodule Diagnoses Made by Physicians**

| | Diagnosis Using 10-mm Slice Thickness | | | |
|---|---|---|---|---|
| Diagnosis Using 2-mm Slice Thickness | NFE | INNFE | NA | Total |
| NFE | 74 | 46 | 10 | 130 |
| INNFE | 67 | 289 | 47 | 403 |
| NA | 1 | 3 | — | 4 |
| Total | 142 | 338 | 57 | 537 |

INNFE, inactive nodule for no further examination; NA, no abnormality; NFE, nodule for further examination.

**TABLE 3. Nodule Groupings and Respective Diagnoses for 2-mm and 10-mm Slice Thickness Images**

| Nodule Group | Diagnoses | Number of Nodules (%) |
|---|---|---|
| 1. Nodule with the same diagnoses for the 2-mm and 10-mm slice thickness images | 2 mm NFE, 10 mm NFE | 74 (13.8) |
| | 2 mm INNFE, 10 mm INNFE | 289 (53.8) |
| 2. Nodules with different diagnoses for the 2-mm and 10-mm slice thickness images | 2 mm NFE, 10 mm INNFE | 46 (8.6) |
| | 2 mm INNFE, 10 mm NFE | 67 (12.5) |
| 3. Nodules that were missed on the 10-mm slice thickness images | 2 mm NFE, 10 mm NA | 10 (1.9) |
| | 2 mm INNFE, 10 mm NA | 47 (8.7) |
| 4. Nodules that were misinterpreted on the 10-mm slice thickness images | 2 mm NA, 10 mm NFE | 1 (0.2) |
| | 2 mm NA, 10 mm INNFE | 3 (0.6) |

INNFE, inactive nodule for no further examination; NA, no abnormality; NFE, nodule for further examination.

the nodules were found in the right upper lobe. Overall, 305, 27, 23, and 182 nodules were located ≤3, >3 to 4, >4 to 5, and >5 mm from the lung border, respectively. Thus, 57% of the nodules were ≤3 mm from the lung border.

### *Statistical Analysis*

The multivariate logistic regression analysis results presented in Table 4 show that a size of >5 mm (odds ratio [OR], 132.50; 95% confidence interval [CI], 14.77–4711), relative

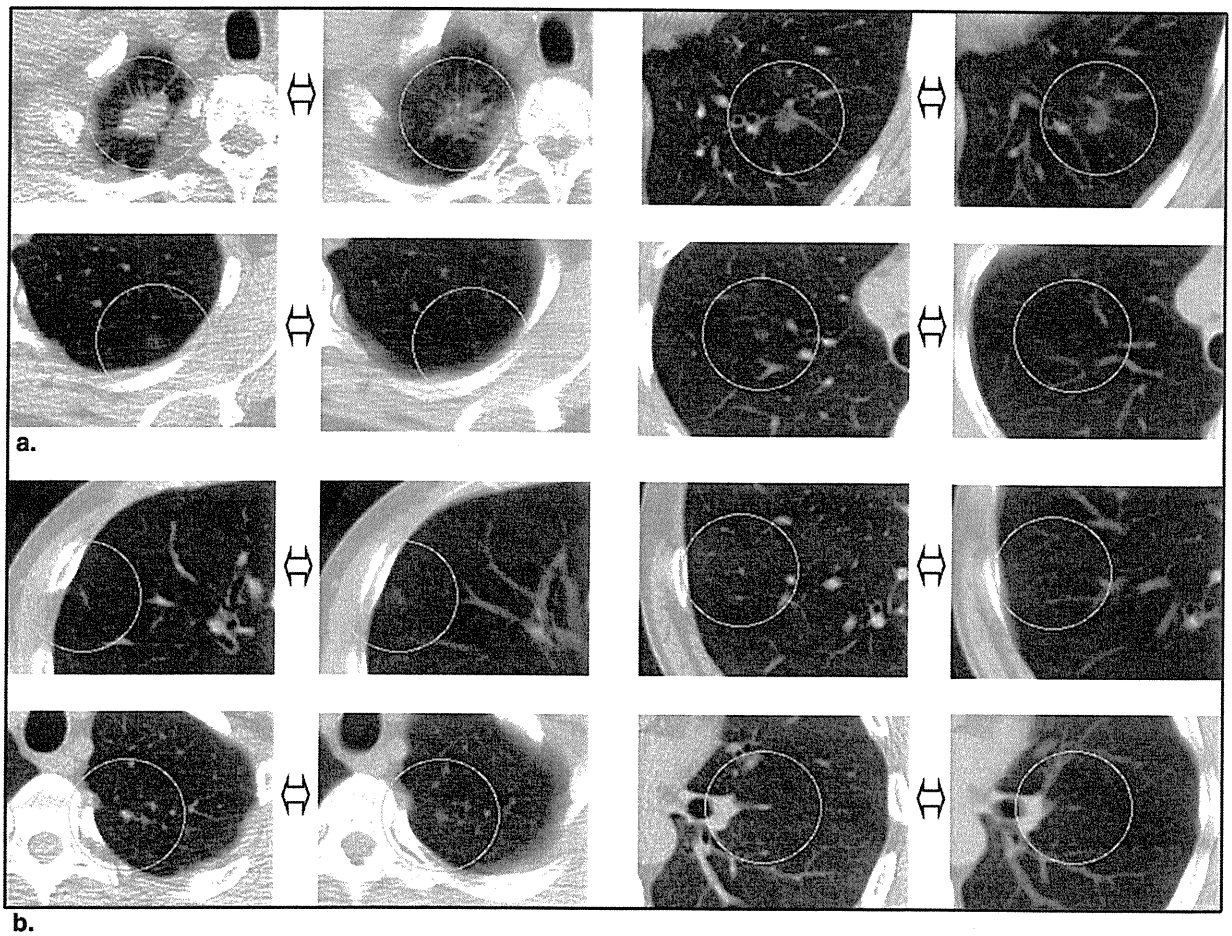


**Figure 3.** Nodules with the same diagnosis using 2-mm slice thickness and 10-mm slice thickness images: **(a)** four lung cancer cases with a diagnosis of 2-mm NFE, 10-mm NFE nodules; **(b)** four cases with a diagnosis of 2-mm INNFE, 10-mm INNFE nodules. INNFE, inactive nodule for no further examination; NFE, nodule for further examination.

to a size of ≤5 mm, and an average CT value of >−700 HU (OR, 27.20; 95% CI, 3.21–645.3), relative to a value of ≤−700 HU, were factors that influenced the detection and nondetection of NFEs. Because of insufficient data, the effect of the location within the lung lobes was not computed. For the INNFE diagnoses shown in Table 5, a size range of 5 mm could not be computed because of an unbalanced distribution of detected and nondetected nodules (≤5 mm, 246 and 47, and >5 mm, 100 and 0, respectively); thus, the size range was changed to 4 mm. A size of >4 mm (OR, 16.10; 95% CI, 6.18–55.19), relative to a size of ≤4 mm, and an average CT value of >−700 HU (OR, 7.67; 95% CI, 2.19–30.91), relative to a value of ≤−700 HU, were factors that influenced the detection and nondetection of INNFEs.

Table 6 shows that a nodule size of >5 mm (OR, 3.60; 95% CI, 1.29–11.04), relative to a size of ≤5 mm, and a distance from the lung border of >3 mm (OR, 2.85; 95% CI, 1.27–6.65), relative to a distance of ≤3 mm, were factors that influenced the diagnostic agreement and disagreement for the NFE diagnoses. A significant association was also shown for nodules located in the right upper lobe (OR, 0.07; 95% CI, 0.003–0.48), relative to nodules located in the right middle lobe. As shown in Table 7, an average CT value of >−700 HU (OR, 11.84; 95% CI, 3.33–55.86), relative to a value of ≤−700 HU, influenced the diagnostic agreement and disagreement for the INNFE diagnoses. A significant influence was also observed for a nodule size of >5 mm (OR, 0.42; 95% CI, 0.25–0.70), relative to a nodule size of ≤5 mm, and a distance from the lung border of >3 mm (OR, 0.41; 95% CI, 0.25–0.66), relative to a distance of ≤3 mm.

## DISCUSSION

We hypothesized that the features and locations of nodules influence the ability of radiologists to detect or not detect nodules and to agree or disagree on the diagnosis. The results of the qualitative diagnosis of six radiologists was quantitatively analyzed to determine the influence of slice thickness (thin and thick sections) using features (sizes and average CT values) and locations (lung lobe location and distance

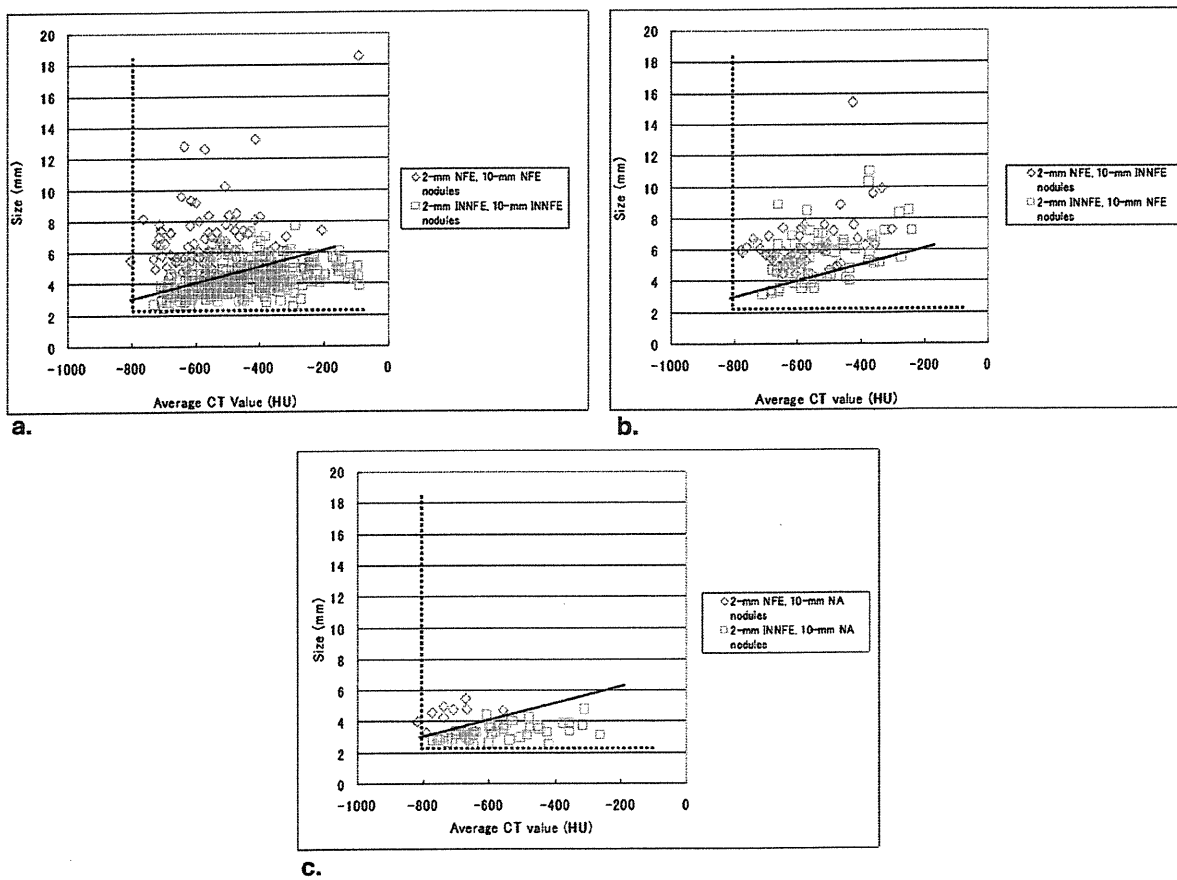


**Figure 4.** Scatterplot showing the average computed tomographic value (Hounsfield units) and nodular size (mm). **(a)** nodules with the same diagnosis using 2-mm and 10-mm slice thickness images. **(b)** nodules with different diagnoses using 2-mm and 10-mm slice thickness images. **(c)** nodules missed on 10-mm slice thickness images.

from the lung border) of nodules. Thick-section images with 10-mm slice thickness were initially used, but thin-section images are mostly used at present. We selected a 10-mm slice thickness for the thick sections and a 2-mm slice thickness for the thin sections.

For detection and nondetection, of the total number of 2-mm NFE diagnoses, 92% were diagnosed as 10-mm NFEs or 10-mm INNFEs. Furthermore, of the total number of 2-mm INNFE diagnoses, 88% were diagnosed as 10-mm INNFEs or 10-mm NFEs. A multivariate logistic regression analysis showed that the average CT value and nodule size of both the NFE diagnoses and the INNFE diagnoses were statistically significant. The OR suggested that size is more significant compared to the average CT value for the detection or nondetection of NFEs and INNFEs. The nodule locations in the lung lobes and the distance from the lung border were not statistically significant.

Regarding diagnostic agreement and disagreement, of the total number of 2-mm NFEs, 57% were diagnosed as 10-mm NFEs. Also, of the total number of 2-mm INNFEs, 72% were diagnosed as 10-mm INNFEs. The multivariate regression analysis showed that for the NFE diagnoses, the nodule size, a nodule location in the right upper lobe (compared to the right middle lobe), and the distance from the lung border were statistically significant. The OR indicated that agreement or disagreement is more likely higher on NFEs with larger size, those located farther from the lung border, and those located in the right upper lobe in comparison to the right middle lobe. The OR indicated that a location in the right upper lobe, compared to the right middle lobe, was the most significant factor. Of the total number of nodules, 57% were ≤3 mm from the lung border, and 35% were found in the right upper lobe. The high percentages show the importance of these factors as influence of slice thickness for diagnosis.

For the INNFE diagnoses, the average CT value, nodule size, and distance from the lung border were statistically significant. Agreement and disagreement on the diagnosis was higher for INNFEs with smaller sizes, higher average CT values, and locations closer to the lung border. The OR indicated that the average CT value is the most significant among these factors.

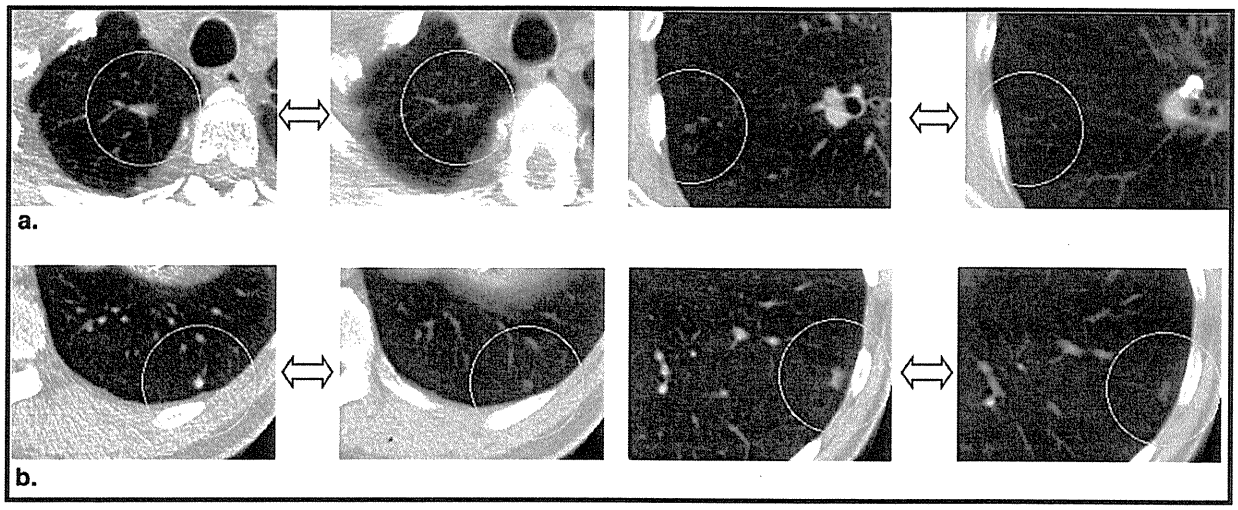


**Figure 5.** Nodules with different diagnoses using 2-mm slice thickness and 10-mm slice thickness images: **(a)** nodules diagnosed as 2-mm NFE, 10-mm INNFE; **(b)** nodules diagnosed as 2-mm INNFE, 10-mm NFE. INNFE, inactive nodule for no further examination; NFE, nodule for further examination.

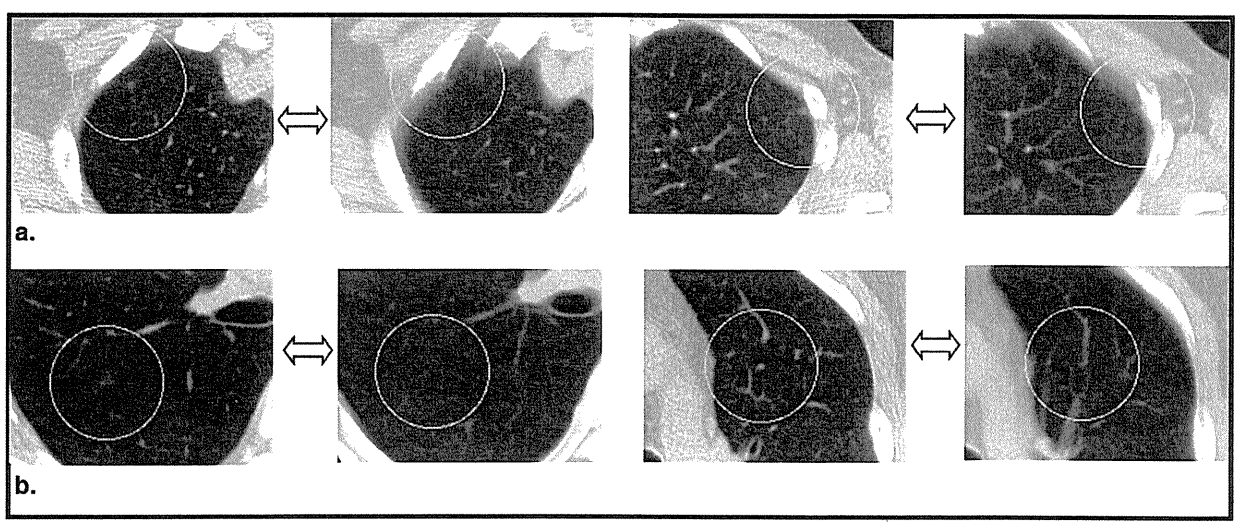


**Figure 6.** Nodules missed on 10-mm slice thickness images: **(a)** nodules diagnosed as 2-mm NFE, 10-mm NA; **(b)** nodules diagnosed as 2-mm INNFE, 10-mm NA. INNFE, inactive nodule for no further examination; NA, no abnormality.

Naidich et al (13) evaluated the factors determining the accuracy of CT imaging for identifying pulmonary nodules. The method consisted of computer-generated nodules on specific portion of the lung that were superimposed on normal CT scans and interpreted by three chest radiologists. Their result revealed that slice thickness, size, nodule location, angiocentricity, and density made a significant contribution in identifying nodules. This was one of the earliest studies dealing with the assessment of the factors affecting pulmonary nodule detection in relation to CT scans. We used actual nodules of the whole lung for evaluation. A study by Fischbach et al (14) analyzed the interpretations of images of the whole lung according to nodule size and diagnostic confidence made by two radiologists using normal-dose CT images of 100 patients. Their results demonstrated an improvement of small nodule detection and confidence levels. Other features and location of nodules that were important factors for diagnosis were not evaluated.

Our study had some limitations. Regarding agreement and disagreement on the diagnosis, the size, average CT value, lung lobe location, and distance from the lung border influenced the NFE and INNFE diagnoses. Other factors, such as nodular shape, surrounding background, and so on, should also be investigated and in future research (24). To prevent

**TABLE 4. Relationships Among Features and Locations of Nodules and Detection or Nondetection of NFEs**

| Parameter | Detected | Nondetected | OR | 95% CI | *P* |
|---|---|---|---|---|---|
| CT value (HU) | | | | | |
| ≤−700 | 16 | 6 | 1.00 | Reference | — |
| >−700 | 104 | 4 | 27.20 | 3.21–645.3 | .0085 |
| Size (mm) | | | | | |
| ≤5 | 14 | 9 | 1.00 | Reference | — |
| >5 | 106 | 1 | 132.50 | 14.77–4711 | .0040 |
| Location* | | | | | |
| Left lower lobe | 26 | 1 | — | — | — |
| Left upper lobe | 19 | 3 | — | — | — |
| Right lower lobe | 31 | 0 | — | — | — |
| Right middle lobe | 12 | 0 | — | — | — |
| Right upper lobe | 32 | 6 | — | — | — |
| Distance from lung border (mm) | | | | | |
| ≤3 | 59 | 6 | 1.00 | Reference | — |
| >3 | 61 | 4 | 7.67 | 0.95–173.88 | .0965 |

Hosmer-Lemeshow test = 0.7076, *df* = 2, *P* = .7022.

CI, confidence interval; CT, computed tomographic; HU, Hounsfield units; NFE, nodule for further examination; OR, odds ratio.

*Lung lobe locations for NFEs were not computed, because of insufficient data.

**TABLE 5. Relationships Among Features and Locations of Nodules and Detection or Nondetection of INNFEs**

| Parameter | Detected | Nondetected | OR | 95% CI | *P* |
|---|---|---|---|---|---|
| CT value (HU) | | | | | |
| ≤−700 | 5 | 8 | 1.00 | Reference | — |
| >−700 | 351 | 39 | 7.67 | 2.19–30.91 | .0020 |
| Size (mm)* | | | | | |
| ≤4 | 132 | 43 | 1.00 | Reference | — |
| >4 | 224 | 4 | 16.10 | 6.18–55.19 | <.0001 |
| Location | | | | | |
| Left lower lobe | 69 | 6 | 0.30 | 0.01–2.22 | .3128 |
| Left upper lobe | 68 | 16 | 0.12 | 0.0058–0.74 | .3916 |
| Right lower lobe | 70 | 6 | 0.23 | 0.01–1.75 | .0598 |
| Right middle lobe | 20 | 1 | 1.00 | Reference | — |
| Right upper lobe | 129 | 18 | 0.17 | 0.008–1.06 | .1163 |
| Distance from lung border (mm) | | | | | |
| ≤3 | 212 | 28 | 1.00 | Reference | — |
| >3 | 144 | 19 | 0.89 | 0.43–1.85 | .7579 |

Hosmer-Lemeshow test = 0.2309, *df* = 2, *P* = .8910.

CI, confidence interval; CT, computed tomographic; HU, Hounsfield units; INNFE, inactive nodule for no further examination; OR, odds ratio.

*The size for INNFE diagnoses was set to 4 mm because of the unbalanced distribution of detected and nondetected nodules for a 5-mm range.

human error in diagnostic reading, a double reading of the images was performed; nevertheless, some errors might still have occurred. Screening data for 360 participants were used for the present analysis, but this study population might not be sufficiently large to make generalizations, particularly regarding the influence of locations within the lung lobes on the detection or nondetection of NFEs. A lack of cancer cannot be assumed in regions with nodules diagnosed as 2-mm INNFE, 10-mm INNFE nodules. Further research using a larger data set, however, might enable the diagnosis of very early stage cancer, such as squamous cell carcinoma or small cell carcinoma, in regions with 2-mm INNFE, 10-mm INNFE nodules.

## CONCLUSIONS

The influence of slice thickness on the ability of radiologists to detect or not detect nodules and to agree or disagree on the diagnosis was quantitatively evaluated. The detection and nondetection of NFEs and INNFEs are influenced by size and average CT value. The agreement and disagreement on NFE and INNFE diagnoses are influenced not only by size

**TABLE 6. Relationships Among Features and Locations of Nodules and Agreement or Disagreement on NFE Diagnosis**

| Parameter | Agree | Disagree | OR | 95% CI | P |
|---|---|---|---|---|---|
| CT value (HU) | | | | | |
| ≤−700 | 10 | 12 | 1.00 | Reference | — |
| >−700 | 64 | 44 | 1.17 | 0.40–3.38 | .7693 |
| Size (mm) | | | | | |
| ≤5 | 7 | 16 | 1.00 | Reference | — |
| >5 | 67 | 40 | 3.60 | 1.29–11.04 | .0177 |
| Location | | | | | |
| Left lower lobe | 19 | 8 | 0.26 | 0.01–1.84 | .2400 |
| Left upper lobe | 9 | 13 | 0.12 | 0.005–0.86 | .0698 |
| Right lower lobe | 19 | 12 | 0.18 | 0.009–1.17 | .1286 |
| Right middle lobe | 11 | 1 | 1.00 | Reference | — |
| Right upper lobe | 16 | 22 | 0.07 | 0.003–0.477 | .0210 |
| Distance from lung border (mm) | | | | | |
| ≤3 | 30 | 35 | 1.00 | Reference | — |
| >3 | 44 | 21 | 2.85 | 1.27–6.65 | .0125 |

Hosmer-Lemeshow test = 4.9741, *df* = 8, *P* = .7603.

CI, confidence interval; CT, computed tomographic; HU, Hounsfield units; NFE, nodule for further examination; OR, odds ratio.

**TABLE 7. Relationships Among Features and Locations of Nodules and Agreement or Disagreement on INNFE Diagnosis**

| Parameters | Agree | Disagree | OR | 95% CI | P |
|---|---|---|---|---|---|
| CT value (HU) | | | | | |
| ≤−700 | 3 | 10 | 1.00 | Reference | — |
| >−700 | 286 | 104 | 11.84 | 3.33–55.86 | .0003 |
| Size (mm) | | | | | |
| ≤5 | 229 | 74 | 1.00 | Reference | — |
| >5 | 60 | 40 | 0.42 | 0.24–0.70 | .0009 |
| Location | | | | | |
| Left lower lobe | 61 | 14 | 0.84 | 0.22–2.80 | .7800 |
| Left upper lobe | 52 | 32 | 0.33 | 0.09–1.02 | .0600 |
| Right lower lobe | 51 | 25 | 0.54 | 0.17–1.88 | .3119 |
| Right middle lobe | 16 | 5 | 1.00 | Reference | — |
| Right upper lobe | 109 | 38 | 0.62 | 0.17–1.88 | .4307 |
| Distance from lung border (mm) | | | | | |
| ≤3 | 189 | 51 | 1.00 | Reference | — |
| >3 | 100 | 63 | 0.41 | 0.25–0.66 | .0002 |

Hosmer-Lemeshow test = 5.7330, *df* = 4, *P* = .2200.

CI, confidence interval; CT, computed tomographic; HU, Hounsfield units; INNFE, inactive nodule for no further examination; OR, odds ratio.

and average CT value but also, importantly, by the locations of nodules.

## REFERENCES


1. Kaneko M, Eguchi K, Ohmatsu H, et al. Peripheral lung cancer: screening and detection with low-dose spiral CT versus radiography. Radiology 1996; 201:798–802.
2. Sone S, Takashima S, Li F, et al. Mass screening for lung cancer with mobile spiral computed tomography scanner. Lancet 1998; 351:1242–1245.
3. Sobue T, Moriyama N, Kaneko M, et al. Screening for lung cancer with low-dose helical computed tomography: Anti-Lung Cancer Association Project. J Clin Oncol 2002; 20:911–920.
4. Sluimer I, Schilham A, Prokop M, et al. Computer analysis of computed tomography scans of the lung: a survey. IEEE Trans Med Imaging 2006; 25:385–405.
5. Henschke CI, Yankelevitz D. CT screening for lung cancer: update 2007. Oncologist 2008; 13:65–78.
6. Henschke CI, McCauley D, Yankelevitz D, et al. Early lung cancer action project: a summary of the findings on baseline screening. Oncologist 2001; 6:147–152.
7. New York Early Lung Cancer Action Project Investigators. CT screening for lung cancer: diagnoses resulting from the New York Early Lung Cancer Action Project. Radiology 2007; 243:239–249.
8. Swensen SJ, Jett JR, Hartman TE, et al. Lung cancer screening with CT: Mayo Clinic experience. Radiology 2003; 226:756–761.
9. Kakinuma R, Kaneko M, Ohmatsu H, et al. Practice of low-dose helical CT screening for lung cancer [article in Japanese]. Respir Circ 2008; 56: 457–463.
10. Nawa T, Nakagawa T, Kusano S, et al. Lung cancer screening using low-dose spiral CT. Chest 2002; 122:15–20.
11. MacMahon H, Austin JH, Gamsu G, et al. Guidelines for management of small pulmonary nodules detected on CT scans: a statement from the Fleischner Society. Radiology 2005; 237:395–400.
12. Japanese Society of CT Screening. Single slice helical CT lung cancer CT screening criteria and guidelines for observation [in Japanese]. Available at: http://www.jscts.org/pdf/guideline/GL0104.pdf. Accessed June 22, 2010.

13. Naidich DP, Rusinek H, McGuiness G, et al. Variables affecting pulmonary nodule detection with computed tomography: evaluation with three-dimensional computer simulation. J Thorac Imaging 1993; 8: 291–299.
14. Fischbach F, Knollmann F, Griesshaber V, et al. Detection of pulmonary nodules by multislice computed tomography: improved detection rate with reduced slice thickness. Eur Radiol 2003; 13:2378–2383.
15. Nishioka D, Kubo M, Kawata Y, et al. The comparative evaluation of lung test based on 2 and 10mm thickness multi-slice CT image. SPIE Med Imaging 2004; 5370:896–903.
16. Sinsuat M, Shimamura I, Saita S, et al. Comparative evaluation of physicians' pulmonary nodule detection with reduced slice thickness at CT screening. SPIE Med Imaging 2008; 6916:691621-1–691621-10.
17. International Commission on Radiological Protection. ICRP publication 103: recommendations of the ICRP. New York: Elsevier, 2008.
18. ImPACT CT patient dosimetry calculator: version 1.0.0. Available at: http://www.impactscan.org. Accessed September 13, 2010.
19. Kanazawa K, Kawata Y, Niki N, et al. Computer-aided diagnosis for pulmonary nodules based on helical CT images. Comput Med Imaging Graph 1998; 22:157–167.
20. Minami K, Kawata Y, Niki N, et al. Classifying pulmonary nodules using dynamic enhanced CT images based on CT number histogram. SPIE Med Imaging 2008; 6915:69152-1–69152-9.
21. Kawai J, Saita S, Kubo M, et al. Automated anatomical labeling algorithm of bronchial branches based on multi-slice CT images. SPIE Med Imaging 2007; 6514. 65143S-1–65143S-8.
22. Saita S, Kubo M, Kawata Y, et al. Algorithm of pulmonary emphysema extraction using thoracic 3-D CT images. SPIE Med Imaging 2008; 6915. 69152L1–69152L8.
23. Hosmer DW, Lemeshow S. Assessing the fit of the model. In: Cressie NAC, Fisher NI, Johnstone IM, et al., eds. Applied Logistic Regression. 2nd ed. Hoboken, NJ: John Wiley, 2000; 143–202.
24. Kawata Y, Niki N, Ohmatsu H, et al. Example-based assisting approach for pulmonary nodule classification in three-dimensional thoracic computed tomography images. Acad Radiol 2003; 10:1402–1415.

# Classification algorithm of lung lobe for lung disease cases based on multi-slice CT images

M. Matsuhiro[*a], Y. Kawata[b], N. Niki[b], Y. Nakano[c], M. Mishima[d], H. Ohmatsu[e], T. Tsuchida[f], K. Eguchi[g], M. Kaneko[f], and N. Moriyama[h]

[a]System Innovation Engineering Graduate School of Advanced Technology and Science The University of Tokushima,
[b]Institute of Technology and Science The University of Tokushima,
[c]Dept.of Respiratory Medicine, Shiga University of Medical Science,
[d]Dept. of Respiratory Medicine, Graduate School of Medicine Kyoto University
[e]National Cancer Center Hospital East,
[f]National Cancer Center Hospital,
[g]Faculty of medicine, Teikyo University,
[h]National Cancer Research Center for Cancer Prevention and Screening,

## ABSTRACT

With the development of multi-slice CT technology, to obtain an accurate 3D image of lung field in a short time is possible. To support that, a lot of image processing methods need to be developed. In clinical setting for diagnosis of lung cancer, it is important to study and analyse lung structure. Therefore, classification of lung lobe provides useful information for lung cancer analysis. In this report, we describe algorithm which classify lungs into lung lobes for lung disease cases from multi-slice CT images. The classification algorithm of lung lobes is efficiently carried out using information of lung blood vessel, bronchus, and interlobar fissure. Applying the classification algorithms to multi-slice CT images of 20 normal cases and 5 lung disease cases, we demonstrate the usefulness of the proposed algorithms.
**Keywords:** multi-slice CT, detection, lung lobe

## 1. INTRODUCTION

With the development of multi-slice CT technology, to obtain an accurate 3D image of lung field in a short time is possible. To support that, a lot of image processing methods need to be developed.
In clinical setting for diagnosis of lung cancer, it is important to study and analyse lung structure, so we developed lung structural analysis system from multi-slice CT images. But our system can't analyse lung disease cases. For diagnosis of lung cancer, lung structural analysis system that can analyse lung disease cases is needed.
In analysis of lung structure, classification of lung lobe provide useful information for preoperative diagnosis of lung transplant from living donors. Classification of lung lobe method was studied many methods[1]-[5]. Extraction of interlobar fissure is important for classification of lung lobe. Interlobar fissure has low density and low contrast on CT images. Therefore, extraction of interlobar fissure for lung disease cases is so difficult. In this report, we describe algorithm which classify lungs into lung lobes for normal cases and lung disease cases from multi-slice CT images using 4D curvature.

## 2. MATERIALS AND METHODS

Medical Imaging 2011: Computer-Aided Diagnosis, edited by Ronald M. Summers, Bram van Ginneken,
Proc. of SPIE Vol. 7963, 796331 · © 2011 SPIE · CCC code: 0277-786X/11/$18 · doi: 10.1117/12.877997

### 2.1 Multi-slice CT data

Our multi-slice CT data are acquired with Toshiba Aquilion. Scan conditions of datasets are shown in Table.1. These 3D images are composed of diaphragm from apex of lung.

Table.1 Scan conditions of normal cases and lung disease cases.

| | Normal Cases | Lung disease cases |
|---|---|---|
| X-ray tube voltage [kV] | 120 | 120 |
| X-ray tube current [mA] | 100-500 | Auto |
| Slice thickness [mm] | 1.0 | 0.5, 1.0 |
| Reconstruction interval [mm] | 1.0 | 0.5, 1.0 |
| Image size [pixels] | 0.647 | 0.625, 0.683 |
| Pixel spacing [mm] | 512x512 | 512x512 |
| The number of cases | 20 | 5 |

### 2.2 Segmentation of thoracic organs

Classification algorithm of lung lobe is described as follows.

#### 2.2.1 Extraction of bronchi, lung field, and pulmonary blood vessel

We extract bronchi using region growing method. We extract lung field and blood vessel using threshold processing.

#### 2.2.2 Classification of lobar bronchi

The space of lobar bronchi is made consists of bronchial branch points of 50 training data . We classify lobar bronchi using the space of lobar bronchi.

#### 2.2.3 Classification lung lobe using lobar bronchi and pulmonary blood vessel

Construction of each space of lobar blood using Delaunay method. The points which are in equal distance from each space of lobar blood vessel are set to boundary, and we classify lung lobe.

#### 2.2.4 Extraction of interlobar fissure

The method of Extraction of interlobar fissure is described as follows.

**step1:** Extraction of interlobar fissure's candidate area using 4D curvature.

Mathematical formulas for calculation of 4D curvature are as follows.

$$F_1 = \begin{pmatrix} 1+f_x^2 & f_x f_y & f_x f_z \\ f_y f_x & 1+f_y^2 & f_y f_z \\ f_z f_x & f_z f_y & 1+f_z^2 \end{pmatrix} \quad (1)$$

$$F_2 = \frac{-1}{\sqrt{D}} \begin{pmatrix} f_{xx} & f_{xy} & f_{xz} \\ f_{xy} & f_{yy} & f_{yz} \\ f_{xz} & f_{yz} & f_{zz} \end{pmatrix} \quad (2)$$

$$D = 1 + (f_x^2 + f_y^2 + f_z^2) \quad (3)$$

$$W = F_1^{-1} F_2 \quad (4)$$

$f_x, f_y, f_z$ are partial differential, $f_{xx}, f_{yy}, f_{zz}, f_{xy}, f_{yz}, f_{zx}$ are second order partial differential, Eigenvalues of W are principal curvatures of 4D curvature. Eigenvectors of W are directional vectors of principal curvatures of 4D curvature. We extract interlobar fissure's candidate area from maximum principal curvature of 4D curvature by threshold processing.

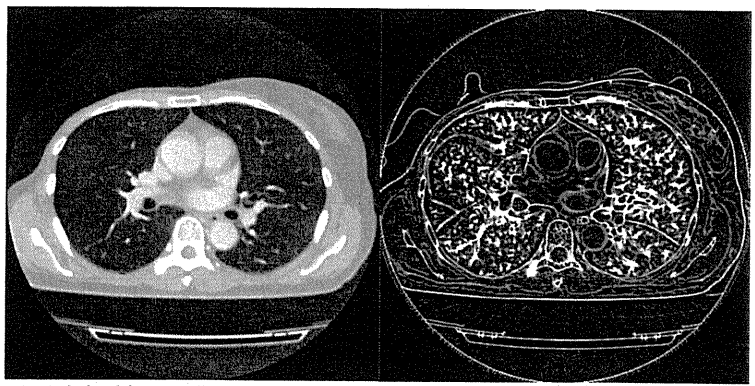

Figure 1. Original image (left), and maximum principal curvature of 4D curvature (right).

**step2:** Surface analysis
The method of surface analysis is described as follows.
(1) Calculation of 3D digital topology
We apply surface thinning interlobar fissure's candidate area. So we calculate 3D digital topology[7]. Arc points are removed. Calculation of normal vector on inner point of surface is obtained by average of directional vectors of maximum principal curvature around inner points of surface.
(2) Classification of surface
The Classification of surface is described as follows
a) Searching for junction point of surfaces.
b) Searching initial point from inner points of surface around junction point of surfaces. We make a peculiar label.
c) Labeling initial point. And Labeling an inner point of surface around initial point when an angle of a normal vector of an inner point of surface around initial point and a normal vector of initial point is small.
d) Initial point move to labeled point by c). We repeat c) till labeling is not possible.
e) We repeat a) to d) till we locate for all junction points.
f) Labeled surfaces are applied average of normal vector.
(3) Grouping of surfaces
Labeled surfaces that connect same junction point of surfaces are grouped when an angle of average of normal vectors is small.

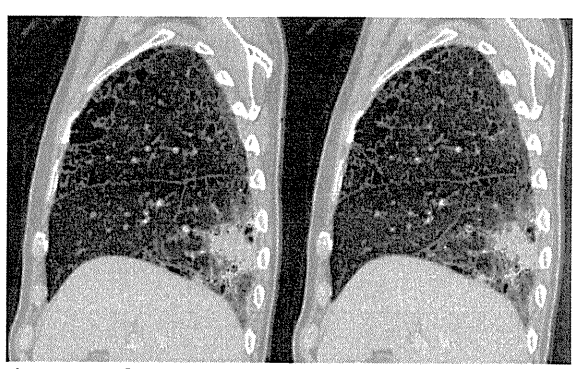

Figure 2. Before grouping (Left), and after grouping (right).

**step3:** Extraction of interlobar fissure
Surfaces of the same group are removed when number of voxels that are surfaces of the same group is small. Each closely attached groups are unified.

**2.2.5 Classification of lung lobe using lobar bronchi, lung blood vessel, and interlobar fissure vessel**
Adjustment around boundary of classified lung lobe using interlobar fissure.

## 3. EXPERIMENTAL RESULTS

We applied the classification algorithms of lung lobe to multi-slice CT images of 20 normal cases and 5 lung disease cases. To evaluate the accuracy of the classified lung lobe, we examined the agreement rate with the manual marking data. The average agreement rates of lung lobe for normal cases and disease cases were shown in Table2. Classification result of lung lobe for disease cases was shown in Figure5.

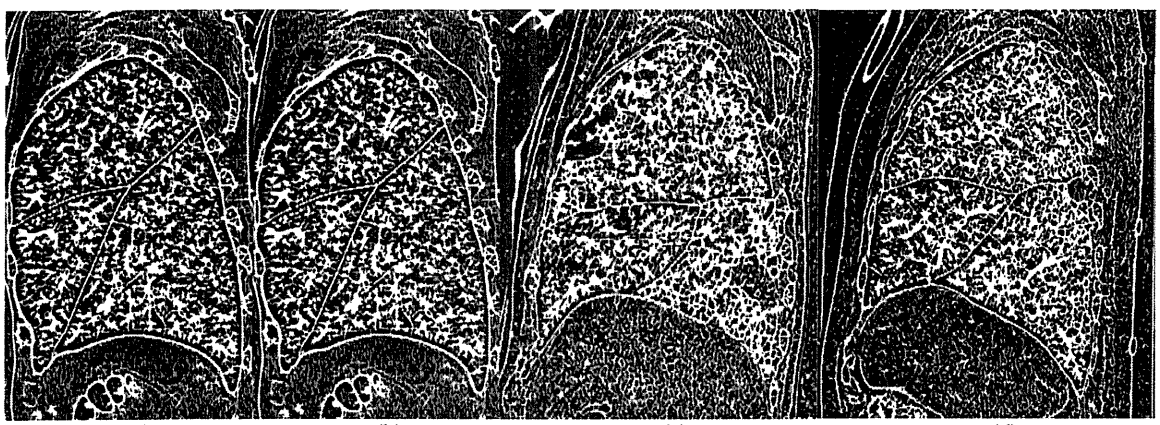

(a) (b) (c) (d)
Figure3. Maximum principal curvature of 4D curvature. (a),(b)Normal cases. (c),(d)Disease cases.

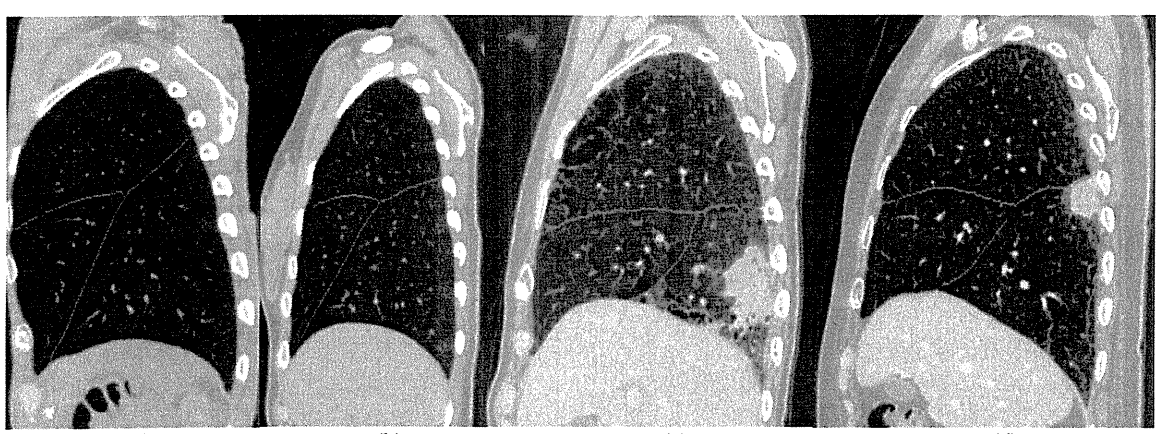

(a) (b) (c) (d)
Figure4. Extraction result of interlobar fissure. (a),(b)Normal cases. (c),(d)Disease cases.